# Application of the
# ENSO Unified Oscillator theory
## to an ocean-only model

**Felicity S. Graham[1,2], Jaclyn N. Brown[2], Andrew Wittenberg[3], Neil J. Holbrook[1]**

**WEALTH FROM OCEANS**
**www.csiro.au**

Conceptual models of ENSO are valuable in understanding the dynamics of ENSO events and the mechanisms involved in the transition between ENSO phases. A unified oscillator conceptual model of the El Niño – Southern Oscillation (ENSO) has been derived from the dynamics and thermodynamics of the coupled ocean-atmosphere system (Wang 2001, hereafter W01). We examine whether the unified oscillator is a good representation of ENSO dynamics. Specifically, we assess the parameters and averaging regions identified for the unified oscillator model. Further, in an attempt to improve the model parameterisations, and also the utility of the model, we fit the unified oscillator to the Geophysical Fluid Dynamics Laboratory (GFDL) Ocean Model version 3.1 (OM3.1) (Griffies *et al.* 2004) and to the Simple Ocean Data Assimilation version 2.1.6 (SODA2.1.6) (Carton *et al.* 2000).

## The unified oscillator

The unified oscillator incorporates four key ENSO conceptual models that describe four delayed negative feedback mechanisms terminating an ENSO event:

- **(i)** locally forced equatorial Kelvin waves in the western Pacific (the western Pacific oscillator; Weisberg and Wang, 1997);
- **(ii)** reflection of off-equatorial Rossby waves at the western boundary (the delayed oscillator; Battisti and Hirst 1989);
- **(iii)** anomalous zonal advection associated with wave reflections at both the eastern and western boundaries (the advective-reflective oscillator; Picaut 1997); and
- **(iv)** gradual discharge of warm water from the equatorial zone, a zonally- and time-integrated effect of the basin-wide wave adjustments (the recharge-discharge oscillator; Jin 1997).

Collectively, Eqs. (1)–(4) below describe the unified oscillator. Eqs. (1) and (2) comprise the positive and negative feedback mechanisms and Eqs. (3) and (4) close the system by relating zonal wind stress anomalies to sea surface temperature (SST) and thermocline anomalies.

**EQUATION 1: TEMPERATURE ANOMALY**

$$\frac{dSST}{dt} = a\tau_1 - b_1\tau_1(t-\eta) + b_2\tau_2(t-\delta) - b_3\tau_1(t-\mu) - \varepsilon SST^3,$$

change in SST = Bjerknes positive feedback + **(ii)** + **(i)** + **(iii)** + damping

**EQUATION 2: THERMOCLINE DEPTH ANOMALY**

$$\frac{dh}{dt} = -c\tau_1(t-\lambda) - R_h h,$$

change in h = **(iv)** + damping

**EQUATION 3: ZONAL WIND STRESS ANOMALY IN NIÑO-4 REGION**

$$\frac{d\tau_1}{dt} = dSST(t+\theta) - R_{\tau 1}\tau_1(t+\theta).$$

**EQUATION 4: ZONAL WIND STRESS ANOMALY IN NIÑO-5 REGION**

$$\frac{d\tau_2}{dt} = eh - R_{\tau 2}\tau_2(t+\alpha)$$

where

SST: Niño-3 sea surface temperature anomaly,

$h$: Niño-6 depth-averaged temperature above 300 m,

$\tau_1$ and $\tau_2$: Niño-4 and Niño-5 zonally-averaged zonal wind stress anomalies respectively,

$a, b_1, b_2, b_3, \varepsilon, c, R_h, d, R_{\tau 1}, e$ and $R_{\tau 2}$, are constants, and $\delta, \eta, \mu, \lambda, \theta$ and $\alpha$ are delay constants.

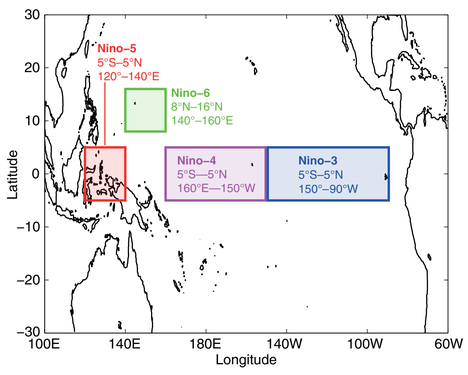


**Figure 1. Averaging regions defined in the unified oscillator.**

## Results

We found optimum parameter values for the unified oscillator by applying a linear least squares analysis on Eqs. (1)–(4) using the OM3.1 and SODA2.1.6 simulations. These empirically-derived values appear to be more appropriate than the theoretical values defined in W01 as well as more consistent between the two data sets (see Table 1). Delay constants were modified from the values in W01 and additional delay terms were introduced into terms on the right-hand sides of Eqs. (3) and (4) to better capture behaviour of the model data and to be consistent with observations (e.g. Meinen and McPhaden 2000). The fitted curves, using the modified parameter values and delay terms (green lines in Figures 2–5), more accurately reproduced the model values (black lines) than the curves with the W01 parameter values and delay terms (red lines). The W01 parameters were up to two orders of magnitude different from the fitted parameters (Table 1).

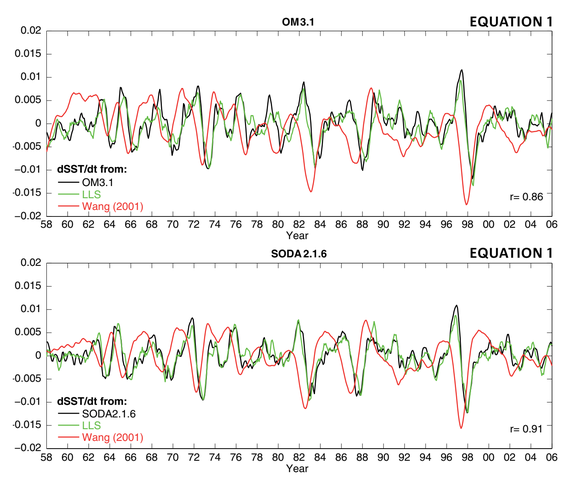


**Figure 2. The black lines in both the upper panel (OM3.1 model) and the lower panel (SODA2.1.6 model) represent the left-hand side of Eq. (1). The green and red lines represent the right-hand side of Eq. (1) with parameter values estimated using linear least squares (green lines) and with the original parameter values from Wang (2001) (red lines). Seasonal cycles were removed from all variables and a low pass filter was applied to remove variability with timescales shorter than 1 year.**

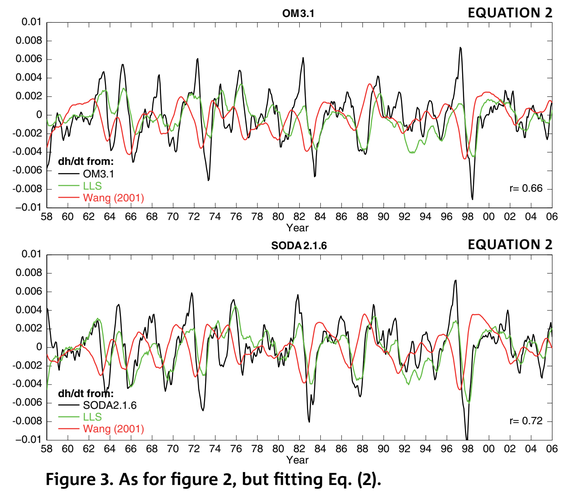


**Figure 3. As for figure 2, but fitting Eq. (2).**

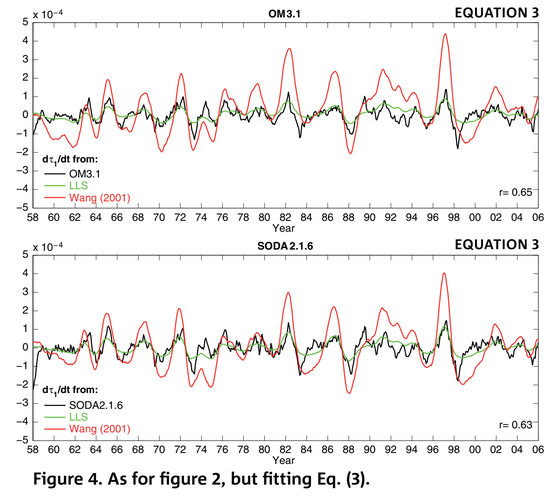


**Figure 4. As for figure 2, but fitting Eq. (3).**

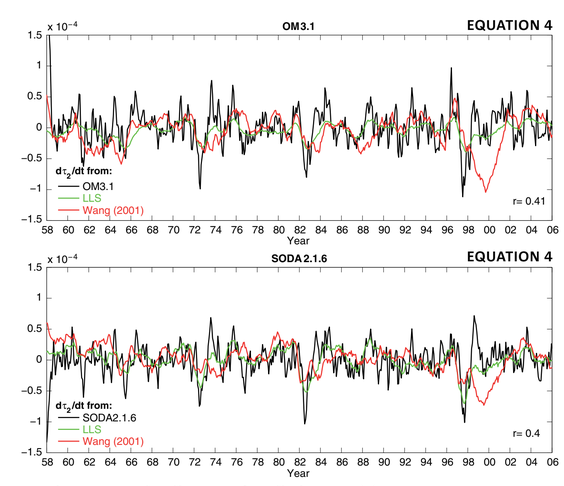


**Figure 5. As for figure 2, but fitting Eq. (4).**

| Parameter (units) | W01 | OM3.1 | SODA2.1.6 |
|---|---|---|---|
| $a$ (°C m² N⁻¹ day⁻¹) | 0.41 | 0.70 | 0.61 |
| $b_1$ (°C m² N⁻¹ day⁻¹) | 0.68 | 0.19 | 0.05 |
| $b_2$ (°C m² N⁻¹ day⁻¹) | 2.1 | 0.078 | 0.16 |
| $b_3$ (°C m² N⁻¹ day⁻¹) | 0.68 | 0.000065 | -0.00025 |
| $\varepsilon$ (°C⁻² day⁻¹) | 0.0033 | 0.54 | 0.58 |
| $c$ (m² N⁻¹ day⁻¹) | 0.0032 | -0.12 | -0.18 |
| $R_h$ (day⁻¹) | 0.0031 | -0.00059 | -0.0024 |
| $d$ (N m⁻² °C⁻¹ day⁻¹) | 0.00010 | -0.000024 | -0.000046 |
| $R_{\tau 1}$ (day⁻¹) | 0.0055 | 0.00088 | 0.000040 |
| $e$ (N m⁻² °C⁻¹ day⁻¹) | 0.000033 | -0.000026 | -0.000026 |
| $R_{\tau 2}$ (day⁻¹) | 0.0055 | 0.00038 | 0.00011 |
| $\delta$ (days) | 30 | 28 | 30 |
| $\eta$ (days) | 150 | 150 | 150 |
| $\mu$ (days) | 90 | 89 | 90 |
| $\lambda$ (days) | 180 | 180 | 180 |
| $\theta$ (days) | 0 | 240 | 270 |
| $\alpha$ (days) | 0 | 180 | 240 |

**Table 1: Original parameter values and delay terms from Wang (2001) and those estimated from the OM3.1 and SODA2.1.6 models using a linear least squares fit of Eqs. (1)–(4).**

The unfitted curve using parameter values from W01 and the fitted curves did not capture the full magnitude of the time-tendencies during ENSO events, or multiple events of the same phase when in succession. The fitted curves for SODA2.1.6 generally explained the variability in that assimilation slightly better than the respective curves for the OM3.1 simulation (see the correlation coefficients r in Figures 2–5).

The dominant regions of variability differed between the phases of ENSO and from the original averaging regions defined in W01 (figures not shown). However, the averaging region for each of the terms was fixed throughout the time period. Hence, the modified unified oscillator was unable to identify whether a particular ENSO event was a weak canonical event or whether it was a stronger event centred in a different location to the canonical ENSO. That the unified oscillator cannot differentiate between ENSO flavours is a major limitation, which impacts on its accuracy in representing ENSO.

## Summary: improvements to the Unified Oscillator

The constant coefficient values for the unified oscillator were optimised using a data assimilation product and an ocean-only model. We further improved the unified oscillator by establishing a new relationship for wind stress dependent on prior ocean states.

## Future challenges

- Determine averaging regions from locations of maximum variability.
- Explore physical implications of modifications to parameter values, delay terms and averaging regions.
- Where modified unified oscillator fits data poorly, determine if additional mechanisms are missing (e.g. noise, nonlinearities).
- How to capture the amplitude of large ENSO events (possibly nonlinear?).
- How to capture El Niños that last more than one year.
- How to capture different ENSO flavours.

### References

Battisti, D. S., and A. C. Hirst, 1989: Interannual Variability in a Tropical Atmosphere-Ocean Model: Influence of the Basic State, Ocean Geometry and Nonlinearity. *Journal of the Atmospheric Sciences*, 46, 25.

Carton, J. A., G. Chepurin, X. Cao, and B. S. Giese, 2000: A Simple Ocean Data Assimilation analysis of the global upper ocean. Part I: Methodology. *Journal of Physical Oceanography*, 30, 311-326.

Griffies, S. M., M. Winton, and B. L. Samuels, 2004: The Large and Yeager (2004) dataset and CORE, 1-5 pp.

Jin, F.-F., 1997: An Equatorial Ocean Recharge Paradigm for ENSO. Part I: Conceptual Model. *Journal of the Atmospheric Sciences*, 54, 19.

Meinen, C. S., and M. J. McPhaden, 2000: Observations of warm water volume changes in the equatorial Pacific and their relationship to El Niño and La Niña. *Journal of Climate*, 13, 9.

Picaut, J., 1997: An Advective-Reflective Conceptual Model for the Oscillatory Nature of the ENSO. *Science (New York, N.Y.)*, 277, 663-666.

Wang, C., 2001: A Unified Oscillator Model for the El Niño-Southern Oscillation. *Journal of Climate*, 14, 98-115.

Weisberg, R.H. and C. Wang, 1997: A Western Pacific Oscillator Paradigm for the El Niño-Southern Oscillation. *Geophysical Research Letters*, 24, 779.

**CONTACT US**
**t** 1300 363 400
+61 3 9545 2176
**e** enquiries@csiro.au
**w** www.csiro.au

**FOR FURTHER INFORMATION**
Felicity S. Graham
**e** felicity.graham@csiro.au
**t** +61 (3) 6232 5283

1 Institute for Marine and Antarctic Studies, University of Tasmania, Hobart Tasmania, Australia
2 Centre for Australian Weather and Climate Research, Wealth from Ocean National Research Flagship. CSIRO Marine and Atmospheric Research, Hobart Tasmania, Australia
3 Geophysical Fluid Dynamics Laboratory, Forrestal Campus, US Route 1, Princeton, NJ USA.

IMAS INSTITUTE FOR MARINE AND ANTARCTIC STUDIES

Australian Government Bureau of Meteorology

The Centre for Australian Weather and Climate Research
A partnership between CSIRO and the Bureau of Meteorology

NOAA U.S. DEPARTMENT OF COMMERCE NATIONAL OCEANIC AND ATMOSPHERIC ADMINISTRATION

Poster layout by Louise Bell, CSIRO Creative Services. January 2012